



**HAL**  
open science

## Reactivity of vadose-zone solids to S-metolachlor and its two main metabolites: case of a glaciofluvial aquifer

Pauline Sidoli, Nicolas Devau, Rafaël Angulo-Jaramillo, Nicole Baran

### ► To cite this version:

Pauline Sidoli, Nicolas Devau, Rafaël Angulo-Jaramillo, Nicole Baran. Reactivity of vadose-zone solids to S-metolachlor and its two main metabolites: case of a glaciofluvial aquifer. *Environmental Science and Pollution Research*, 2020, 27 (18), pp.22865-22877. 10.1007/s11356-020-08579-6 . hal-03013933

**HAL Id: hal-03013933**

**<https://univ-lyon1.hal.science/hal-03013933>**

Submitted on 7 Jan 2021

**HAL** is a multi-disciplinary open access archive for the deposit and dissemination of scientific research documents, whether they are published or not. The documents may come from teaching and research institutions in France or abroad, or from public or private research centers.

L'archive ouverte pluridisciplinaire **HAL**, est destinée au dépôt et à la diffusion de documents scientifiques de niveau recherche, publiés ou non, émanant des établissements d'enseignement et de recherche français ou étrangers, des laboratoires publics ou privés.

[Click here to view linked References](#)

# 1    **Reactivity of vadose zone solids to S-metolachlor and its two main metabolites: case of a** 2    **glaciofluvial aquifer**

3    Pauline Sidoli (1), Nicolas Devau (1), Rafael Angulo Jaramillo (2), Nicole Baran (1),

4    <sup>(1)</sup> BRGM, 3 Avenue Claude Guillemin, BP 36009, 45060 Orléans Cedex 2

5    <sup>(2)</sup> LEHNA UMR 5023 CNRS ENTPE Université Claude Bernard- Lyon 1, Rue Maurice Andin, F-69518 Vaulx-  
6    en-Velin

7    Corresponding author : Pauline Sidoli- [p.sidoli@brgm.fr](mailto:p.sidoli@brgm.fr) +33(0)238644607

8

## 9    **ABSTRACT:**

10    The vulnerability of groundwater to pesticides is governed in part by sorption mechanisms in the vadose zone,  
11    commonly studied in soil but less well known in the geological solids. To alleviate this lack of knowledge,  
12    adsorption of the herbicide S-metolachlor (SMOC), and of two of its metabolites—metolachlor ethane sulfonic  
13    (MESA) and metolachlor oxanilic acid (MOXA)— were studied with batch equilibrium method on seventeen  
14    surface soils and three geological solids of the vadose zone overlying a glaciofluvial aquifer. In grainsize terms,  
15    the latter three were sand for the first two samples and gravel for the third. Adsorption is ordered as follows:  
16    SMOC>>MESA>MOXA, except for one of the geological solids for which MESA adsorption was slightly  
17    higher than that of SMOC ( $K_d = 0.73$  vs.  $0.44$  L kg<sup>-1</sup>). The low MOXA adsorption could only be quantified for  
18    the gravel sample ( $K_d = 0.74$  L kg<sup>-1</sup>), which was also more reactive than all the other samples to MESA and  
19    SMOC ( $K_d = 2.08$  and  $28.8$  L kg<sup>-1</sup>, respectively). Statistical multivariate tests related the highest  $K_d$  values for  
20    SMOC with the soils and geological solids with the highest organic-carbon and clay-fraction contents. The  
21    highest  $K_d$  values for MESA were found in the samples containing high oxide concentrations. Our results shed a  
22    new light on the adsorption of SMOC, MESA and MOXA suggesting that during their transfer to groundwater,  
23    pesticides and metabolites can be adsorbed in the vadose zone on both soils and geological solids.

24

25    **Keywords** (6 à 8): *adsorption, pesticide, chloroacetanilide, metolachlor ESA, metolachlor OXA, groundwater,*  
26    *geological solids, reactivity*

27

28 **Acknowledgments:**

29 This study received financial support from BRGM and the Rhône-Méditerranée-Corse Water Agency, as part of  
30 the PENATH Project. We thank our BRGM colleagues who contributed to the work, and in particular L. Gourcy,  
31 N. Maubec for the DRX analyses and G. Wille for the MEB work. H.M. Kluijver translated and edited the final  
32 version of the paper.

33

## 34 **1. Introduction**

35 The contamination of groundwater by pesticides is a well known problem affecting many aquifers in numerous  
36 countries (Kolpin et al. 1998a; Postigo and Barcelo 2015; Toccalino et al. 2014). The European Water  
37 Framework Directive (2000/60) and its sister Directive (2006/118/CE) set the objectives to be reached for the  
38 protection and conservation of groundwater masses. More generally, the protection of water resources and the  
39 monitoring of groundwater quality is an issue to be treated at a world-wide scale, particularly where groundwater  
40 is used for drinking. Today, many questions remain concerning the velocity with which contaminants are  
41 transferred to groundwater, and its corollary of evaluating the risk of seeing contaminants re-appear years after  
42 their application.

43 The mobility of pesticides in vadose (unsaturated) zone, and hence their transfer to groundwater compartment,  
44 depends on the degradation and sorption processes on solid particles, well described for soils in the literature  
45 (Arias-Estevez et al. 2008; Dubus et al. 2003). Until now, it has been assumed that pesticides and/or their  
46 metabolites flushed from the soil will interact only little with geological solids in the underlying vadose zone  
47 because of their low organic matter content, meaning that their transfer to groundwater is essentially controlled  
48 by the hydrological conditions of aquifer recharge. Other work, though patchy, has shown that pesticides can  
49 react with geological solids in the vadose zone (Baran and Gourcy 2013; Clausen et al. 2004; Coquet 2003;  
50 Coquet et al. 2004; Janniche et al. 2010; Madsen et al. 2000; Papiernik et al. 2006; Sidoli et al. 2016a). As an  
51 example among these previous studies, Sidoli et al. 2016a showed that transfer of herbicide S-metolachlor in  
52 glaciofluvial solids is delayed compared to water tracer because of sorption processes. It is therefore essential to  
53 collect data on how pesticides are adsorbed on geological solids of the vadose zone, to understand if interactions  
54 in geological solids are negligible or contrary significant compared to the transfer through soil and thus if they  
55 are matters or not for risk analysis or even quantitative solute transport simulations.

56 The few data available on the adsorption of metabolites in the vadose zone is a major hindrance for  
57 understanding how such molecules are transferred. The differences in physico-chemical properties between the  
58 metabolites and their parent molecule may cause a difference in reactivity to the solids in soil and the vadose  
59 zone. Such a change of physico-chemical properties between mother molecule and metabolites is observed for  
60 several pesticides, including metolachlor. This pesticide is electrically neutral whereas its two metabolites are  
61 negatively charged to the environmental pH. Metolachlor, applied as a mixture enriched in S isomer (S-  
62 metolachlor), is a selective herbicide used in particular on maize. Introduction of S-metolachlor (SMOC) in some

63 countries in replacement of rac-metolachlor (racemic mixture of R- and S- isomers) was motivated by its higher  
64 herbicide efficiency (Blaser et al. 2007; Shaner et al., 2006). Metolachlor is massive used worldwide, and is one  
65 of the most common organic compounds found in groundwaters in North America (Toccalino et al. 2014), in  
66 Europe (Loos et al. 2010) and in France (Lopez et al. 2015). The retention of SMOC in soil is moderate and  
67 mainly linked to organic matter content (Alletto et al. 2013; Baran and Gourcy 2013; Bedmar et al. 2011; Weber  
68 et al. 2003). SMOC can also be adsorbed on geological solids, as was shown by the batch equilibrium method on  
69 alluvial deposits (Baran and Gourcy 2013) and by column-percolation tests on glaciofluvial deposits (Sidoli  
70 et al. 2016a). Metolachlor ethane sulfonic acid (MESA) and metolachlor oxanilic acid (MOXA) are commonly  
71 quantified in groundwater at concentrations over that of metolachlor and which can reach 4,8 and 3,8  $\mu\text{g L}^{-1}$   
72 respectively (Amalric et al. 2013; Baran and Gourcy 2013; Hancock et al. 2008; Hladik et al. 2008; Kolpin et  
73 al. 1998b, 2004; Postle et al. 2004; Steele et al. 2008). The metabolites MESA and MOXA have very low  
74 adsorption coefficients in soil (Krutz et al. 2004) and are more mobile in unsaturated media than their parent  
75 molecule (Baran and Gourcy 2013; Sidoli et al. 2016a). However, the key parameters involved in the adsorption  
76 of MESA and MOXA in soil are unknown. Few data exist for the adsorption of SMOC on geological solids in  
77 the vadose zone, and almost nothing is known about the adsorption of MESA and MOXA in the vadose zone.  
78 For those reasons, the role played by geological solids of the vadose zone in the transfer of pesticides and their  
79 metabolites is difficult to establish today without more data on adsorption values.

80 The purpose of this study was to improve our understanding of role played by the vadose zone in retaining  
81 SMOC and its two metabolites MESA and MOXA. Our specific objectives are i) to quantify and compare the  
82 adsorption of all three molecules on soils and on geological solids collected in the vadose zone of a glaciofluvial  
83 aquifer and ii) to determine the factors governing molecular adsorption. Adsorption measurements ( $K_d$  values)  
84 were lead with batch laboratory experiments at equilibrium. We used multivariate analyses for linking the  $K_d$   
85 values with soil and solid properties, to determine the factors governing molecular adsorption.

## 86 **2. Materials and methods**

### 87 **2.1. S-metolachlor and its two main metabolites**

88 The experiments were performed with S-metolachlor (purity  $\geq 99.5\%$ ) purchased from Dr Ehrenstorfer  
89 (Augsburg, Germany), and MESA (purity  $\geq 96.2\%$ ) and MOXA (purity  $\geq 97.9\%$ ) from Sigma-Aldrich  
90 (Steinheim, Germany) (Table 1). Individual standard stock solutions of SMOC, MESA and MOXA ( $500 \text{ mg L}^{-1}$ )

91 were prepared on a weight basis in methanol and stored at -20 °C. Solutions used for spiking samples were  
92 prepared in a  $\text{CaCl}_2$   $10^{-2}$  M aqueous solution with ultrapure water (MilliQ® Merck Millipore) and stored at 4 °C.

93 SMOC, MESA and MOXA concentrations were determined with an Acquity ultra-performance liquid  
94 chromatography system (UPLC™, Waters) interfaced to a triple quadrupole mass spectrometer (Quattro Premier  
95 XE/Q, Waters). Online extraction was done with an SPE cartridge (Oasis HLB-Column 25  $\mu\text{m}$ ).  
96 Chromatographic separation was done with a Waters Acquity UPLC BEH C18 column (2.1 mm x 150 mm,  
97 particle size 1.7  $\mu\text{m}$ ). Mecoprop-d3 and simazine-d10 were used as internal standards for metabolite and  
98 metolachlor analyses, respectively. The quantification limit was 0.025  $\mu\text{g L}^{-1}$  for metolachlor and 0.050  $\mu\text{g L}^{-1}$   
99 for both MESA and MOXA. The analytical method developed for off-line extraction is described in detail in  
100 Amalric et al (2013).

## 101 **2.2. Sampling site**

102 The sampling site is located in a Quaternary glaciofluvial deposit (Würm age) of about 110  $\text{km}^2$ , east of Lyon,  
103 France. The regional aquifer is from 30 to 70 m thick and the water table is between 2 and 40 m below the soil  
104 surface. Seventeen surface soils were sampled in different agricultural plots at up to 30 cm depth. The soils are  
105 loamy to sandy-loamy characterized by large amounts of amorphous iron- and aluminium oxides (mean values  
106 2.7 and 1.8  $\text{g kg}^{-1}$ , respectively). They are chromic cambisols according to the WRB classification system  
107 (2006). Sampling strategy and physico-chemical properties of the surface soils were described by Sidoli et  
108 al. (2016b) and in Table 2.

109 The glaciofluvial solids (GFS) were collected in a quarry, several metres above the water table and 30 m below  
110 ground surface. Two main lithofacies were earlier identified and sampled on site based on grain-size distribution  
111 (Goutaland et al. 2008, 2013; Lassabatere et al. 2010; Sidoli et al. 2016a).

## 112 **2.3. Glaciofluvial solids analysis**

113 The particle size distributions of the two main lithofacies are, for one, a bimodal mixture of gravel and sand with  
114 grain sizes up to 100 mm diameter (Gcm,b) and, for the other, sand with grain sizes between 0 and 2 mm (S-x)  
115 (Goutaland et al. 2008). After air-drying, both samples (S-x and Gcm,b lithofacies) were sieved at 0 to 2 mm  
116 particle sizes (S-x and Gcm,b [0,2]). A coarser sieving diameter (2 to 10 mm particle size) was used on the  
117 bimodal gravel (Gcm,b [2,10]).

118 For S-x, Gcm,b [0,2] and Gcm,b ]2,10], the following chemical properties were analysed:  $\text{pH}_{\text{KCl}}$ ,  $\text{pH}_{\text{water}}$   
119 (AFNOR 10390 (2005)), CEC Metson (AFNOR X 31.130 (1999)), total organic carbon content (AFNOR 10694  
120 (1995a)), available phosphate (Olsen P) (AFNOR 11263, 1995), crystallized oxy-hydroxides ( $\text{Fe}_{\text{DCB}}$  and  $\text{Al}_{\text{DCB}}$ )  
121 based on the Mehra-Jackson method (1960), and amorphous oxy-hydroxides ( $\text{Fe}_{\text{Tamm}}$  and  $\text{Al}_{\text{Tamm}}$ ) based on the  
122 Tamm method (1992). The experimental pH, hereafter referred to as ' $\text{pH}_{\text{CaCl}_2}$ ', was measured in batch  
123 supernatants with a pH microelectrode (Inlab Flex-Micro).

124 Mineralogical compositions were determined by X-ray diffraction (XRD) measurements with a Bruker D8  
125 Advance diffractometer, equipped with a  $\text{CuK}\alpha$  source ( $\lambda=1.5418 \text{ \AA}$ ) operating at 40 kV and 40 mA, and a  
126 Lynx-Eye 1D detector. XRD patterns were collected from  $5^\circ$  to  $90^\circ 2\theta$ , with a step of  $0.02^\circ 2\theta$  and a time step of  
127 139.2 s. XRD diffraction patterns were interpreted with DIFFRAC.Plus EVA software. SIROQUANT™  
128 quantitative X-ray diffraction analysis software processed the XRD spectra for quantifying the mineral phases.  
129 Quantification was done with the Rietveld method.

130 Sample porosity was measured by mercury-porosimetry analyses (Auropore IV 9500 Micromeritics). The S-x,  
131 Gcm,b [0,2] and Gcm,b ]2,10] samples were quartered in order to obtain representative test samples of 5 to 7 g.  
132 The sample porosity was measured on six replicates for Gcm,b]2,10] and on two replicates for S-x and Gcm,b  
133 [0,2].

#### 134 **2.4. SEM analysis**

135 Samples S-x, Gcm,b [0,2] and Gcm,b ]2,10] were observed by scanning electron microscopy on a Tescan  
136 Mira3XMU SEM with an Edax Pegasus EDS (Electron Dispersive X-ray Spectroscopy) microanalysis system  
137 using an Edax ApolloXPP Silicon Drift Detector (SDD) (resolution 126 eV @ Mn Ka) and EDS Edax TEAM  
138 software. The samples were observed at different high-tension values (15 or 25 kV) adapted to the analyses. A  
139 long acquisition time of 100 to 500 sec., with a counting rate of several thousand cps, was used for acquiring  
140 EDS spectra in order to detect elements at several tenths of a percent. The Gcm,b ]2,10] gravels were stuck on  
141 aluminium pin stubs with a conducting carbon lacquer (PELCO® water-based graphite paint from Ted Pella).  
142 The samples S-x and Gcm,b [0,2] were stuck by pressure on a conductive carbon adhesive (double coated  
143 PELCO Tabs™ carbon conductive tabs, Ted Pella). The samples were then covered with a 10 nm carbon layer,  
144 using a carbon evaporator under a secondary vacuum (Cressington 208 Carbon) to ensure that the surface would  
145 be conductive.

## 146 **2.5. Adsorption experiments**

147 Adsorption experiments were run according to a normalized method (OECD guideline 106, 2000). The tests  
148 were run for a liquid/solid ratio of 1. Four grams of S-x and Gcm,b [0,2] solids were used. For Gcm,b [2,10], the  
149 experiments were done with 10 g in order to obtain repeatable replicates despite the high heterogeneity of this  
150 material. Dried solid samples were hydrated with a CaCl<sub>2</sub> background solution electrolyte. Dehydrated calcium  
151 chloride (CaCl<sub>2</sub>), purity ≥98%, was purchased from Merck. The hydration was done 16 h before spiking to reach  
152 near-equilibrium conditions. Spiking was done with a pesticide solution diluted in 0.01M CaCl<sub>2</sub>, shaken in a  
153 head-over-head agitator at 20 °C in a dark box. Based on a kinetic study (data not shown), the equilibrium  
154 adsorption experiments were conducted for 24 h for the seventeen surface soils, S-x and and Gcm,b [0,2], and  
155 for 72 h in the case of Gcm,b [2,10]. Equilibrium adsorption was measured from a unique initial pesticide  
156 concentration of 1 mg L<sup>-1</sup>. After centrifugation at 3000 rpm for 30 min and filtration through a 0.22 μm acetate  
157 cellulose filter, the supernatants were analysed for SMOC, MESA or MOXA concentrations.

158 The amount of pesticide adsorbed on the solid phase ( $Q_e$ , mg kg<sup>-1</sup>) was calculated as the difference between  
159 initial concentration and equilibrium concentration ( $C_e$ , mg L<sup>-1</sup>). The distribution between the amount adsorbed  
160 on solids and the supernatant concentration at equilibrium was expressed with the distribution coefficient  $K_d$  (L  
161 kg<sup>-1</sup>), calculated with Equation (1)

$$162 \quad Q_e = K_d C_e \quad (1)$$

163 Solids blanks included in the experiments do not show any contamination of the samples before the experiments.  
164 No adsorption was measured on tubes and filters used for batch experiments. Molecule stability in solution was  
165 tested for the duration of the experiments, revealing any loss of molecules. Each experiment was carried out in  
166 triplicate.

## 167 **2.6. Statistical analysis**

168 Due to the nature of the dataset, usual statistical analyses such as multiple regression done to quantify  
169 relationship between sorption properties of pesticides and/or metabolites and physico-chemical properties of soil  
170 could not be used in the present study. Indeed, these statistical analyses are not suitable for small dataset, which  
171 is the case notably for the GFS sub-dataset (Legendre and Legendre, 1998). To overcome this limit,  
172 unsupervised and supervised ordination analyses were performed. Unsupervised analysis enables us to explain

173 how soil and GFS samples could be distinguished according to their physicochemical properties and how these  
174 properties are linked between them. Supervised analysis was devoted to determine how the physico-chemical  
175 properties of soils and GFS could explain their reactivity towards sorption of SMOC and MESA but not for  
176 MOXA as the amount of adsorbed MOXA could not be quantified. More details on these tools are given below.

177 First, a principal component analysis (PCA) was run to ordinate the 17 soils and the 3 GFS for each according to  
178 the following physico-chemical variables: 1) pH measured in  $\text{CaCl}_2$ , water and KCl solutions ( $\text{pH}_{\text{CaCl}_2}$ ,  $\text{pH}_{\text{water}}$ ,  
179  $\text{pH}_{\text{KCl}}$ ); 2) cationic exchange capacity (CEC); 3) solid texture (clay, silt and sand contents); 4) total organic  
180 carbon (Organic C) 5) phosphorus contents extracted by the Olsen method (Olsen P); 6) contents in poorly  
181 crystallized aluminium ( $\text{Al}_{\text{ox}}$ ) and iron ( $\text{Fe}_{\text{ox}}$ ) oxides, and contents in well crystallized aluminium and iron oxides  
182 ( $\text{Al}_{\text{DCB}}$  and  $\text{Fe}_{\text{DCB}}$ , respectively). This unsupervised exploratory method allowed finding the best low-  
183 dimensional representation of the variance associated with physico-chemical variables. Relationships between  
184 observations and physico-chemical variables were investigated through the analysis of how such variables  
185 contribute to the calculated principal components. Before doing so, the variables were centred and scaled. The  
186 results were presented as a correlation circle for the physico-chemical variables and a biplot build on the two  
187 principal axes to illustrate the ordination of the samples. The PCA was done on two distinct datasets, one  
188 gathering both soil and GFS and the other focusing only on soil materials, to determine whether the GFS with its  
189 specific physico-chemical properties could be analysed together with the soil material.

190 Then, a partial least squares linear discriminant analysis (PLS-DA) was done. This supervised multivariate  
191 analysis computes the best discriminating functions based on the physico-chemical properties of the samples to  
192 distinguish the  $K_d$  values measured on each of them. This statistical analysis was done for SMOC and MESA,  
193 respectively. This statistical test implies first to group soil and GFS samples based on the values of the  $K_d$   
194 measured. For this purpose, we used a cumulative distribution function built from measured  $K_d$  values either for  
195 SMOC or MESA. Based on the cumulative distribution function, the first and third quantile values as well as the  
196 median values were calculated. These values were then used to separate measured  $K_d$  values into four groups,  
197 enabling us to transform the two quantitative variables—corresponding to  $K_d$ -value measurements for SMOC  
198 and MESA—into two categorical (discrete) variables. The first group,  $K_d_1$ , combines the  $K_d$  values below the  
199 first quantile. The second group,  $K_d_2$ , is for the  $K_d$  values above the first quantile and below the median,  
200 whereas the third group,  $K_d_3$ , consists of the  $K_d$  values above those of the second rank and below the third  
201 quartile. The remaining  $K_d$  values were aggregated into a fourth group,  $K_d_4$ .

202 The same physico-chemical variables than those used in the PCA were integrated in the discriminant analysis.  
203 These variables were transformed into latent variables based on a partial least squares regression algorithm that  
204 searched for maximum covariance, representing the relevant sources of data variability with linear combinations  
205 of the original variables. The plots used to present the results are similar to those used for PCA. A confusion  
206 matrix comparing the *a priori* (real) and *a posteriori* (calculated) classification of the observations was  
207 calculated using the cross-validation technique.

208 To complete the results from the PLS-DA, a non-parametric MANOVA based on permutation algorithm was run  
209 on the dataset to statistically evaluate whether the whole physico-chemical properties of the soil or GFS are  
210 statistically different according to the four groups derived from the  $K_d$  measurements done either on SMOC or  
211 MESA, respectively. A Bray-Curtis similarity matrix was calculated on data that had been scaled and centred. A  
212 permutation matrix for calculating pseudo-F ratios was built using Markov Chain Monte Carlo methods (999  
213 permutations). This multivariate approach was conducted with and without accounting for GFS in the dataset, to  
214 determine whether the results for soils and GFS could be interpreted simultaneously or not. In addition, a non-  
215 parametric Kurskal-Walis test was used on each of the 13 physico-chemical variables measured on samples by  
216 accounting also for the categorical variable derived from measurement on sorption of SMOC or MESA,  
217 respectively. In case of a significant difference, a Conover-Iman *post-hoc* test was done to identify which groups  
218 differ from the others. This univariate approach was conducted in similar way that the non-parametric  
219 MANOVA (presence or not of GFS). Results are shown in Appendix B. All statistical analyses were carried out  
220 with R 3.4.2 software (R Development Core Team, 2017). The FactoMineR, MASS and mixOmics libraries  
221 were used.

222

## 223 3. Results and discussion

### 224 3.1. Variability of the properties of vadose-zone solids

225 The first two PCA axes allow a correct description of much of the variance inherent in the soil and GFS  
226 observations as determined from their physico-chemical properties (Fig. 1). The inertia associated with these  
227 first two axes is 81%. Analysis of the variance/covariance matrix shows that the first axis is constructed by the  
228 following physico-chemical variables:  $\text{pH}_{\text{KCl}}$ ,  $\text{pH}_{\text{water}}$ ,  $\text{pH}_{\text{CaCl}_2}$ ,  $\text{CaCO}_3$ , Clay, Silt, CEC,  $\text{Al}_{\text{ox}}$ ,  $\text{Fe}_{\text{ox}}$  and Organic C.

229 This first axis correctly separates the GFS points from soils, in particular those with a high calcium carbonate  
230 content ( $\geq 178 \text{ g kg}^{-1}$  Table 2)—mainly calcite (Table 3)—, associated with high pH values. Compared to GFS,  
231 the surface soils are decarbonated with lower pH values (mean  $\text{pH}_{\text{CaCl}_2}$  value of 5.9 vs.  $\geq 7.2$ ) and a higher Organic C  
232 (mean value of 13.6 vs.  $\leq 2.5 \text{ g kg}^{-1}$ ), higher clay contents (mean value of 13.2% vs.  $\leq 4.2\%$ ) and higher  $\text{Al}_{\text{ox}}$  and  
233  $\text{Fe}_{\text{ox}}$  contents (mean values of 1.8 and 2.7 vs.  $\leq 0.7$  and  $\leq 1.2 \text{ g kg}^{-1}$ , respectively) (Table 2). More details on the  
234 soils are given in (Sidoli et al 2016a). The second axis has a lower inertia and is constructed by the Olsen P,  
235  $\text{Al}_{\text{DCB}}$  and  $\text{Fe}_{\text{DCB}}$  variables, but does not provide a clear separation between the soils, except for soils 11, 13 and 2  
236 that have different physico-chemical properties. Compared to the other soils, 2 and 13 have the lowest P Olsen  
237 ( $\leq 5.6 \text{ mg kg}^{-1}$ ) and highest  $\text{Al}_{\text{DCB}}$  contents (11.1 and  $10.6 \text{ g kg}^{-1}$ , respectively). Moreover, except for soil 18, soils  
238 13 and 11 have the highest Organic Carbon contents ( $\geq 16.1 \text{ g kg}^{-1}$ ).

239 The GFS mineralogy as determined by XRD analyses mostly consists of quartz ( $>32\%$ ) and calcite ( $>18\%$ )  
240 (Table 3). To a lesser extent, feldspars, such as albite (sodic plagioclase) and microcline (potassic feldspar), and  
241 clay minerals (smectite, kaolinite and chlorite) are present as well, as are illite-type minerals, illite *sensu stricto*  
242 and/or micas. No trace of Fe or Al oxy-hydroxides was detected by DRX analyses, even though significant Fe  
243 and Al concentrations were measured with the Mehra-Jackson ( $\text{Fe}_{\text{DCB}}$  and  $\text{Al}_{\text{DCB}}$ ) and Tamm ( $\text{Fe}_{\text{ox}}$  and  $\text{Al}_{\text{ox}}$ )  
244 extraction methods. These contrasting results indicate that Fe and Al oxy-hydroxides must be present, but that  
245 their abundances in the mineralogical assemblages of the three fractions are low. The abundance of the main  
246 mineral phases, quartz and calcite, is different between fraction S-x and the fractions Gcm,b[0,2] and  
247 Gcm,b[2,10]. Fraction S-x is richer in quartz (54% vs.  $\leq 36\%$ ), but calcite is less abundant (18% vs. 30 and 34%)  
248 compared to the two Gcm,b fractions. No difference was apparent between the minor mineral phases in the three  
249 fractions. Even though no mineralogical analysis was made of the soils, it is probable that they consist of an  
250 assemblage of goethite, inherited clays of the smectite and illite types, potassic feldspars, ferro-magnesian micas

251 and quartz, similar to the mineralogy of other, geographically close, fersiallitic soils, formed over glacio-fluvial  
252 materials and in the same stage of pedological evolution (Bornand 1978).

### 253 **3.2. $K_d$ values in the vadose zone profile**

254 In soils, the  $K_d$  distribution coefficients of SMOC fall between 2.34 and 6.32 L kg<sup>-1</sup> (Table 4), a normal range of  
255  $K_d$  values as earlier measurements on different soil types provided a range of 1.02 to 8.7 L kg<sup>-1</sup> (Alletto et  
256 al. 2013; Cassigneul et al. 2018; Krutz et al. 2004; Seybold and Mersie 1996; Vryzas et al. 2007; Weber et  
257 al. 2003). Regarding the metabolites, the  $K_d$  values are very low for MESA ( $K_d < 0.75$  L kg<sup>-1</sup>) and below the  
258 detection limit for MOXA (Table 4). The few available studies on these metabolites also showed very low  
259 adsorption on soils, for MESA  $K_d$  values below 0.19 L kg<sup>-1</sup> (Kupfersberger et al. 2018). The adsorption on the  
260 soils we studied follows the same decreasing order: SMOC >> MESA > MOXA, whereas Krutz et al. (2004)  
261 mentioned comparable  $K_d$  values for MESA and MOXA in a clayey soil (average  $K_d$  value of 0.75 and  
262 0.77 L kg<sup>-1</sup>, respectively). This adsorption difference might be due to the clayey nature of the soil, which may  
263 have favoured the MOXA adsorption process.

264 For the S-x and Gcm,b [0,2] samples, the  $K_d$  values for SMOC were lower than those for the soils, with 0.44 and  
265 0.57 L kg<sup>-1</sup>, respectively. The adsorption coefficients for MESA were 0.73 and 0.46 L kg<sup>-1</sup>, respectively, within  
266 the 0.03 and 0.74 L kg<sup>-1</sup> range we measured for soils. MOXA does not seem to sorb with the solid phases in S-x  
267 and Gcm,b[0,2]. These results are coherent with an earlier study on the fine [0,2] mm fraction of other  
268 sedimentary geological solids, that measured very low adsorption of MESA and no adsorption of MOXA (Baran  
269 and Gourcy, 2013). Finally, the adsorption properties of the [2,10] mm fraction of Gcm,b are quite different from  
270 the two fine fractions of S-x and Gcm,b[0,2]), as the former fraction appears to be very reactive for SMOC,  
271 MESA and MOXA. The measured  $K_d$  values were 28.8, 2.08 and 0.74 L kg<sup>-1</sup>, respectively. The coarse  
272 [2,10] mm fraction of the Gcm,b lithofacies thus has a much higher retention capacity for SMOC, MESA and  
273 MOXA than Gcm,b [0,2] and S-x, but also higher than those of the 17 soils studied. The adsorption order of the  
274 molecules is SMOC > MESA > MOXA for the solids of the vadose zone, except for facies S-x where MESA  
275 adsorption is slightly higher than that of SMOC. These results complete data obtained earlier during column-  
276 transfer experiments for the same solids (Sidoli et al. 2016a), with an identical adsorption order.

277

### 278 **3.3. Key factors for adsorption on vadose-zone solids**

#### 279 **3.3.1. Adsorption of SMOC**

280 A discriminant analysis of the physico-chemical properties of the solids (soil and GFS) for the SMOC adsorption  
281 values ( $K_d$ ) identified four value groups Kd\_1, Kd\_2, Kd\_3 and Kd\_4. In a univariate analysis (ANOVA), the  
282 solids for which the  $K_d$  values are over the median (Kd\_3 and Kd\_4 groups) have significantly higher Organic C  
283 contents than the solids of group Kd\_1 (Appendix A). The solids of group Kd\_4 also have a statistically higher  
284 CEC content than those of group Kd\_1.

285 It should be noted that the sand fraction in the grainsize assemblage is significantly lower in the Kd\_4 group  
286 solids than in those of group Kd\_1. The latter, though, have lower crystallized aluminium oxide (Al extracted  
287 with the CDB method) as well as lower amorphous aluminium- and iron oxide contents (Al and Fe extracted  
288 with the ammonium oxalate method) than the other groups. Such differences in  $Al_{CDB}$  contents are, however,  
289 only significant in the solids of group Kd\_3. Notwithstanding these correlations, this approach can only link the  
290  $K_d$  values to the physico-chemical properties of the solids on an individual basis. This consideration may be the  
291 simplest view of the relationship between sorption processes and solids properties, which probably interact with  
292 each other.

293 Therefore, the permANOVA aims at determining which collective physico-chemical properties have a  
294 significant effect on the  $K_d$  values of SMOC; it shows that over 77% of the intra-group variance can be explained  
295 by the first two discriminant axes (Fig. 2). The physico-chemical properties that contribute to these two axes  
296 suffice for determining a significant difference between the groups, as was seen from the permANOVA results  
297 that indicated a significant difference between groups. Most of the variance is explained by the first discriminant  
298 axis constructed from the variables Clay,  $Fe_{ox}$ ,  $Al_{ox}$  Organic C, CEC and Silt, which correctly distinguishes three  
299 units (Kd\_1, Kd\_4 and the Kd\_2 + Kd\_3 unit) (65%). The variance associated with the second axis is only 13%.  
300 Analysis of the correlation circle (Fig. 2) confirms the results from the univariate approach (Appendix A),  
301 showing that the solids in group Kd\_1 stand out from the others by textures with less clay and silt,  
302 concentrations of weakly crystallized iron and aluminium oxides, less Organic C and a lower CEC. The second  
303 discriminant axis distinguishes groups Kd\_1, Kd\_2 and Kd\_3 from group Kd\_4. The Olsen P, Sand,  $Al_{DCB}$  and  
304  $Fe_{DCB}$  variables are the main contributors to this axis. The solids with the highest affinity for SMOC (Kd\_4  
305 group solids) contain phosphorus concentrations and higher concentrations of well-crystallized iron oxides

306 ( $Fe_{DCB}$ ) than the other solids; they also contain less well-crystallized aluminium oxide and have a relatively  
307 depleted sand fraction.

308 The results obtained from a PLS-DA analysis, only considering data obtained from soil samples, are similar  
309 (Appendix B2), indicating that the soil- and GFS data can be processed in the same way. This implies that the  
310 mechanisms controlling the fate of SMOC are similar in soils and GFS.

311 The important role played by the organic-carbon content in SMOC sorption, shown by this study, had already  
312 been mentioned in earlier work on soils (Alletto et al. 2013; Baran and Gourcy 2013; Bedmar et al. 2011;  
313 Kodesova et al. 2011; Patakioutas and Albanis 2002; Sanchezcamazano et al. 1995; Si et al. 2009; Vryzas et al.  
314 2007; Weber et al. 2003; Wood et al. 1987), but no work on geological solids had been reported as far as we  
315 know. Cwielag-Piasecka et al. (2018) showed that metolachlor is strongly adsorbed on humic acids extracted  
316 from soil. The earlier correlations between SMOC adsorption and clay content (Baran and Gourcy 2013; Si et  
317 al. 2009; Vryzas et al. 2007; Weber et al. 2003) and CEC (Si et al. 2009) were incorporated in our statistical  
318 work. In soil, organic matter and clays are arranged in a specific manner with oxides-hydroxides within organo-  
319 metallic complexes. This specific arrangement probably explains why iron- and aluminium oxides contribute to  
320 discriminating the  $K_d$  variance, even though no correlation between SMOC- and oxide adsorption is shown by  
321 classic univariate tests. The interactions between S-metolachlor and organic matter might be the result of  
322 hydrogen interaction (Liu et al. 2000, 2002) showed that the adsorption of chloroacetanilide herbicides (alachlor,  
323 acetochlor, propachlor, metolachlor) on the constituents of organic matter occurs through the formation of a  
324 hydrogen bond between the carbonyl ( $-C=O$ ) and/or nitrogen (C-N) groups of the herbicides and the carboxyl  
325 and protonated hydroxyl groups of humic acids. The adsorption of chloroacetanilides on clays would be related  
326 to the formation of hydrogen bonds with water molecules directly present on the surface of clay platelets, or with  
327 water molecules that hydrate the exchangeable cations on platelet surfaces (Bosetto et al. 1993; Li et al. 2006;  
328 Liu et al. 2000; Pusino et al. 1992). As the three molecules we studied are part of this family, it is possible that  
329 the adsorption mechanisms are similar to those described in the above-mentioned studies.

### 330 *3.3.2. Adsorption of the anionic metabolites MESA (ESA-metolachlor) and MOXA (OXA-* 331 *metolachlor)*

332 A discriminant analysis shows that over 78% of the intra-group variance can be explained by the first two  
333 discriminant axes (Fig. 3). Most (65%) of the variance is explained by the first discriminant axis, the variance

334 associated with the second axis being only 13%. The first axis is mostly constructed by the variables Clay, Fe<sub>ox</sub>,  
335 Al<sub>ox</sub>, Organic C and Silt. The parameters Fe<sub>DCB</sub>, Al<sub>DCB</sub> and pH<sub>CaCl2 - water</sub> and <sub>KCl</sub> contribute to both the first and  
336 second axes. Even so, neither axis provides a significant distinction between the four groups Kd\_ESA\_1,  
337 Kd\_ESA\_2, Kd\_ESA\_3, and Kd\_ESA\_4, as is outlined by the permANOVA results that show no significant  
338 difference between the groups. Analysis of the correlation circle confirms the univariate results, showing that the  
339 solids (soils or GFS) are not distinguished between the K<sub>d</sub> groups when considering the physico-chemical  
340 properties separately (Appendix A). The solids (soils or GFS) for which the K<sub>d</sub> values are highest (group  
341 Kd\_ESA\_4) thus do not have significantly higher physico-chemical properties than the solids of the three other  
342 groups Kd\_ESA\_1, Kd\_ESA\_2 and Kd\_ESA\_3. To summarize, the physico-chemical properties governing the  
343 adsorption of MESA on GFS and soils cannot be identified in a significant manner.

344 The results obtained from a PLS-DA analysis when considering only the data from soil samples are similar  
345 (Appendix B3), indicating that GFS and soil data can be processed in the same way. This result also implies that  
346 the mechanisms controlling MESA adsorption are similar in soil and GFS. Only few data were published on  
347 MESA adsorption coefficients in soil (Baran and Gourcy 2013; Krutz et al. 2004) and no adsorption mechanisms  
348 were described for this metabolite.

349 Nevertheless, we can question the potential role of iron- and aluminium oxides, and of clays, on MESA  
350 adsorption in soils and GFS. With a pK<sub>a</sub> of 1.8 (Table 1), MESA effectively is an anionic molecule with respect  
351 to the surrounding pH values. And, the adsorption of anionic molecules in soil is known to occur on protonated  
352 hydroxyl groups on oxide surfaces and clay-platelet edges (MacKay and Vasudevan 2012). As the gradients in  
353 contents of iron- and aluminium oxides are very slight between the different groups of soil or GFS solids  
354 (Kd\_ESA\_1, Kd\_ESA\_2, Kd\_ESA\_3 and Kd\_ESA\_4, Appendix A), their role in the adsorption of MESA is  
355 probably masked in the PLS-DA statistical analysis, the results appearing to be non-significantly different.

356 pH contributes to the correlation circle (Fig. 3). Its impact is on the oxide charges, but it has no effect on the  
357 MESA charge as the negative charge of the molecule conferred by the sulfonate group is constant under the  
358 environmental pH (Table 1).

359 Concerning MOXA, no adsorption value could be determined for either surface soils, or the fine fractions  
360 [0,2] mm of GFS (S-x and Gcm,b[0,2]), adsorption appearing to be extremely limited. No statistical analysis  
361 could be carried out on the single K<sub>d</sub> value obtained for Gcm,b[2,10]. No description was found in the literature

362 concerning the parameters governing its adsorption. Even though both MOXA and MESA are anionic molecules  
363 at environmental pH (pKa of 1.8 and 4.8, respectively, Table 1), their adsorption is different in the solids of the  
364 vadose zone. As is suspected for MESA, iron oxy-hydroxides might play a role in adsorbing the anionic MOXA  
365 molecule, even though this is very slight, or even unmeasurable, in our study. The nature of the functional  
366 grouping of the negatively charged molecule might be at the origin of the difference in adsorption between the  
367 two molecules. MESA has an anionic sulfonate group that may be more reactive to the protonated hydroxyl  
368 groups of oxides and clays than the anionic carboxyl group of MOXA. This hypothesis is supported by work that  
369 showed that, on the surface of goethite, the affinity constant of the carboxylic group ( $\log K=1.26$ ; (Filius et  
370 al. 1997) is much weaker than the affinity constant of a sulphate ( $\log K=19.5$ ; (Geelhoed et al. 1997)). Such  
371 affinity constants are coherent with the adsorption order of MESA and MOXA observed on the soil or GFS  
372 solids of our study.

### 373 **3.4. Influence of the GFS adsorption interface on herbicide adsorption**

374 In the permANOVA analysis, the  $K_d$  variance between the different groups of solids was studied using physico-  
375 chemical property contents, in order to identify the mechanisms involved in SMOC and MESA adsorption. As is  
376 standard when identifying the adsorption of pesticides in soil, the next step would be to draw up the pedotransfer  
377 rules that lead to predictive values for adsorption (Wauchope et al. 2002; Weber et al. 2004). The fact of  
378 considering the total sample mass in pedotransfer rules can be criticized when dealing with a soil rich in  
379 aggregates, where pesticide molecules would not have access to the central part of the aggregate (Wauchope et  
380 al. 2002); in fact, such an approach would not be representative of the real composition of the soil/pesticide  
381 interface available for adsorption. For such fluvioglacial solids with low porosity (<2%, Table 3), the adsorption  
382 interface is smaller. Therefore, it is impossible to draw up predictive adsorption values for SMOC, MESA and  
383 MOXA when using only physico-chemical mass properties measured via general analyses of a solid. For a  
384 quantitative prediction of the adsorption of these molecules, one should consider the adsorption interface on the  
385 surface of the solids rather than their overall composition, which, by itself, is insufficient for a precise  
386 understanding of their reactivity.

387 For this reason, we carried out MEB-EDS analyses to complete the mineralogical and other data, in order to  
388 understand if potentially reactive mineral phases might be present on the surfaces of fluvioglacial solids. We  
389 identified iron oxides on the surface of S-x, Gcm,b [0,2] and Gcm,b[2,10] grains (Fig. 4). The morphology of  
390 these iron oxides and/or -hydroxides on the surface of the S-x and Gcm,b [0,2] samples seems relatively similar,

391 with dimensions of about a dozen microns, whereas those on the surface of Gcm,b]2,10] are much smaller—  
392 around one micron—and assembled in clusters.

393 However, without more mineralogical information on the nature of these oxides, we can draw no conclusions on  
394 differences in reactivity. The clay platelets on the surface of Gcm,b]2,10] grains could also adsorb SMOC.  
395 Concerning S-x and Gcm,b[0,2], no clays were observed, but the MEB-EDS analyses were not exhaustive. The  
396 higher adsorption of SMOC, MESA and MOXA on Gcm,b ]2,10] could be explained by either a different  
397 chemistry, or by a different structural arrangement of the clay minerals, iron oxides and reactive organic matter,  
398 more favourable for the adsorption of molecules than that of the adsorption interfaces of Gcm,b[0,2] and S-x.

399 Thus, rather than the content in overall mineral and organic phases of the solid, it may be the difference in  
400 chemistry and reactivity at the adsorption interface that should be looked for and defined. This new approach  
401 should lead to a more precise explanation of the adsorption differences between solids and, more generally, to  
402 the construction of future predictive models of the adsorption of pesticides and their metabolites for both soils  
403 and geological solids.

#### 404 **4. Conclusions**

405 The adsorption properties in the vadose zone of the herbicide S-metolachlor (SMOC) and its ethane sulfonic  
406 (MESA) and oxanilic acid (MOXA) metabolites, were measured on surface soils as well as on heterogeneous  
407 geological solids. The latter are glaciofluvial (GFS) deposits with grain sizes ranging from sand (samples S-x  
408 and Gcm,b[0,2]) to gravel (Gcm,b]2,10]).

409 The adsorption coefficients  $K_d$  are variable, from low values (0.03 to 2.08 L kg<sup>-1</sup>) to values below the detection  
410 limits for the metabolites, and from low to high values for SMOC (0.44 to 28.8 L kg<sup>-1</sup>). For all three molecules,  
411 gravel is the most reactive solid matrix of the vadose zone. These variations of adsorption in soils and GFS seem  
412 to be mainly related to the presence and reactivity of iron oxides for the negatively charged molecules MESA  
413 and MOXA. For the neutral molecule SMOC, the highest  $K_d$  values were measured on solids with higher organic  
414 matter contents and reactivity values than the others, even in the case of GFS. Clay minerals also contribute to  
415 increasing the reactivity of solids in the vadose zone for SMOC adsorption.

416 In view of our results showing the importance of the solid/liquid interface in characterizing the reactivity of GFS  
417 for SMOC and its metabolites, it is probable that—even when increasing the number of samples—it would not

418 be possible to apply pedotransfer rules. In fact, as the geological solids have a very low to nil porosity, the  
419 physico-chemical parameters taken as a whole do not reflect the physico-chemical composition of the SMOC  
420 adsorption interface and of that of its metabolites. It is thus essential to define the spatial distribution and  
421 reactivity of the mineral and organic phases located at the reactive adsorption interface, in order to arrive at a  
422 precise definition of the sorption capacity of complex solid matrices, such as GFS.

423 We provide new data on the adsorption of SMOC, MESA and MOXA on geological solids of the vadose zone.  
424 In addition, we have added to the few available data on soils for both MESA and MOXA. Geological solids are  
425 often hardly considered when studying pollutant transfer to groundwater, but our work shows that such relatively  
426 deep solids can be more reactive than the surface horizons of soils. Integrating the sorption parameters of  
427 pesticides and their metabolites on geological solids in predictive transfer models will lead to a more precise  
428 estimate of the transfer time of molecules to groundwater, leading in turn to a more reliable long-term  
429 monitoring of the changes in groundwater quality.

430 In short, refining the temporal predictions of groundwater quality, will improve the suitability and quality of  
431 management measures.

432

433

434

435 **References:**

436 AFNOR (1995) Soil quality- Determination of organic and total carbon after dry combustion (elementary  
437 analysis). NF ISO 10694.

438 AFNOR (1995) Soil quality- Determination of phosphorus- Spectrometric determination of phosphorus soluble  
439 in sodium hydrogen carbonate solution. NF ISO 11263.

440 AFNOR (1999) Soil quality- Chemical methods- Determination of cationic exchange capacity (CEC) and  
441 extractible cations. NF X 31-130.

442 AFNOR (2005) Soil quality- Determination of pH. NF ISO 10390.

443 Amalric L, Baran N, Coureau C, Maingot L, Buron F, Routier S (2013) Analytical developments for 47  
444 pesticides: first identification of neutral chloroacetanilide derivatives in French groundwater. *International*  
445 *Journal of environmental analytical chemistry* 93: 1660-1675

446 Alletto L, Benoit P, Bolognesi B, Couffignal M, Bergheaud V, Dumény V, Longueval C, Barriuso E (2013).  
447 Sorption and mineralisation of S-metolachlor in soils from fields cultivated with different conservation tillage  
448 systems. *Soil and tillage research* 128: 97-103

449 Arias-Estevez M, Lopez-Periago E, Martinez-Carballo E, Simal-Gandara J, Mejuto J-C, Garcia-Rio L (2008)  
450 The mobility and degradation of pesticides in soils and the pollution of groundwater resources. *Agriculture*  
451 *Ecosystems and Environment* 123: 247-260.

452 Baran N, Gourcy L (2013) Sorption and mineralization of S-metolachlor and its ionic metabolites in soils and  
453 vadose zone solids: Consequences on groundwater quality in an alluvial aquifer (Ain Plain, France). *Journal of*  
454 *contaminant hydrology* 154: 20-28

455 Bedmar F, Daniel PE, Costa JL, Gimenez D (2008) Sorption of acetochlor, S-metolachlor and atrazine in surface  
456 and subsurface soil horizons of Argentina. *Environmental toxicology and chemistry* 30: 1990-1996

457 Blaser HU, Pugin B, Spindler F, Thommen M (2007) From a chiral switch to a ligand portfolio for asymmetric  
458 catalysis. *Accounts of Chemical Research* 40: 1240-1250

459 Bornand M. (1978) Altération des matériaux fluvio-glaciaires, genèse et évolution des sols sur terrasses  
460 quaternaires dans la moyenne vallée du Rhône. Rapport de thèse de l'Université des Sciences et Techniques du  
461 Languedoc, Montpellier, France. 327p.

462 Bosetto M, Arfaioli P, Fusi P (1993) Interactions ofalachlor with homoionic montmorillonites. Soil science 155:  
463 105-113

464 Cassigneul A, Benoit P, Nobile C, Bergheaud V, Dumeny V, Etievant V, Maylin A, Justes E, Alletto L (2018)  
465 Behaviour of S-metolachlor and its oxanilic and ethane sulfonic acids metabolites under fresh vs. partially  
466 decomposed cover crop mulches: A laboratory study. Science of the total environment 631-632: 1515-1524

467 Clausen L, Larsen F, Albrechtsen HJ (2004) Sorption of the herbicide dichlobenil and the metabolite 2,6-  
468 dichlorobenzamide on soils and aquifer sediments. Environmental science and technology 38: 4510-4518

469 Coquet Y (2003) Sorption of pesticides atrazine, isoproturon, and metamitron in the vadose zone. Vadose zone  
470 journal 2: 40-51

471 Coquet Y, Ribiere C, Vachier P (2004) Pesticide adsorption in the vadose zone: a case study on Eocene and  
472 Quaternary materials in Northern France. Pest management science 60: 992-1000

473 Cwielag-Piasecka I, Medynska-Juraszek A, Jerzykiewicz M, Debicka M, Bekier J, Jamroz E, Kawalko D (2018)  
474 Humic acid and biochar as specific sorbents of pesticides. Journal of soils and sediments 18: 2692-2702

475 Dubus IG, Brown CD, Beulke S (2003). Sources of uncertainty in pesticide fate modelling. Science of the Total  
476 Environment 317: 53-72

477 Filius JD, Hiemstra T, Van Riemsdijk WH (1997) Adsorption of small weak organic acids on goethite: modeling  
478 of mechanisms. Journal of colloid and interface science 195: 368-380

479 Geelhoed JS, Hiemstra T, VanRiemsdijk WH (1997) Phosphate and sulfate adsorption on goethite: Single anion  
480 and competitive adsorption. Geochimica et cosmochimica acta 61: 2389-2396

481 Goutaland D, Winiarski T, Lassabatere L, Dube JS, Angulo-Jaramillo R (2013) Sedimentary and hydraulic  
482 characterization of a heterogeneous glaciofluvial deposit: Application to the modeling of unsaturated flow.  
483 Engineering geology 166: 127-139

484 Goutaland D, Winiarsky T, Dubé JS, Bièvre G, Buoncristiani JF, Chouteau M, Giroux B (2008)  
485 Hydrostratigraphic characterization of glaciofluvial deposits underlying an infiltration basin using ground  
486 penetrating radar. *Vadose zone journal* 7: 14

487 Hancock TC, Sandstrom MW, Vogel JR, Webb RMT, Bayless ER, Barbash JE (2008). Pesticide fate and  
488 transport throughout unsaturated zones in five agricultural settings, USA. *Journal of environmental quality* 37: 3

489 Hladik ML, Bouwer EJ, Roberts AL (2008) Neutral degradates of chloroacetamide herbicides: occurrence in  
490 drinking water and removal during conventional water treatment. *Water research* 42: 4905-4914

491 Janniche GS, Mouvet C, Albrechtsen HJ (2010) Acetochlor sorption and degradation in limestone subsurface  
492 and aquifers. *Pest management science* 66: 1287-1297

493 Kodesova R, Kocarek M, Kodes V, Drabek O, Kozak J, Hejtmankova K (2011) Pesticide adsorption in relation  
494 to soil properties and soil type distribution in regional scale. *Journal of hazardous materials* 186: 540-550

495 Kolpin DK, Schnoebelen DJ, Thurman EM (2004) Degradates provide insight to spatial and temporal trends of  
496 herbicides in ground water. *Ground water* 42: 601-608

497 Kolpin DW, Barbash JE, Gilliom RJ (1998a) Occurrence of pesticides in shallow groundwater of the United  
498 States: Initial results from the National Water-Quality Assessment Program. *Environmental science and*  
499 *technology* 32: 558-566

500 Kolpin DW, Thurman EM, Linhart SM (1998b) The environmental occurrence of herbicides: the importance of  
501 degradates in ground water. *Archives of environmental contamination and toxicology* 35: 385-390

502 Krutz LJ, Senseman SA, McInnes KJ, Hoffman DW, Tierney DP (2004) Adsorption and desorption of  
503 metolachlor and metolachlor metabolites in vegetated filter strip and cultivated soil. *Journal of environmental*  
504 *quality* 33(3): 939-945

505 Kupfersberger H, Klammler G, Schuhmann A, Bruckner L, Kah M (2018) Modeling subsurface fate of S-  
506 metolachlor and metolachlor ethane sulfonic acid in the westliches leibnitzer feld aquifer. *Vadose zone journal*  
507 17: 12.

508 Lassabatere L, Angulo-Jaramillo R, Goutaland D, Letellier L, Gaudet JP, Winiarski T, Delolme C (2010) Effect  
509 of the settlement of sediments on water infiltration in two urban infiltration basins. *Geoderma* 156: 316-325.

510 Legendre P, Legendre L, (1998) *Numerical ecology, Developments in Environmental Modelling* 20. Elsevier  
511 Science

512 Li H, Teppen BJ, Laird DA, Johnston CT, Boyd SA (2006) Effects of increasing potassium chloride and calcium  
513 chloride ionic strength on pesticide sorption by potassium- and calcium-smectite. *Soil science society of*  
514 *America journal* 70: 1889-1895

515 Liu WP, Gan JY, Papiernik SK, Yates SR (2000) Structural influences in relative sorptivity of chloroacetanilide  
516 herbicides on soil. *Journal of agricultural and food chemistry* 48.

517 Liu WP, Gan JY, Yates SR (2002) Influence of herbicide structure, clay acidity, and humic acid coating on  
518 acetanilide herbicide adsorption on homoionic clays. *Journal of agricultural and food chemistry* 50: 4003-4008

519 Loos R, Locoro G, Comero S, Contini S, Schwesig D, Werres F, Balsaa P, Gans O, Weiss S, Blaha L, Bolchi M,  
520 Gawlik BM (2010) Pan-European survey on the occurrence of selected polar organic persistent pollutants in  
521 ground water. *Water research* 44: 4115-4126

522 Lopez B, Ollivier P, Togola A, Baran N, Ghestem JP (2015) Screening of French groundwater for regulated and  
523 emerging contaminants. *Science of the total environment* 518: 562-573

524 MacKay AA, Vasudevan D (2012) Polyfunctional ionogenic compound sorption: challenges and new  
525 approaches to advance predictive models. *Environmental science and technology* 46: 9209-9223

526 Madsen L, Lindhardt B, Rosenberg P, Clausen L, Fabricius I (2000) Pesticide sorption by low organic carbon  
527 sediments: a screening for seven herbicides. *Journal of environmental quality* 29: 1488-1500

528 Mehra OP, Jackson ML (1960) Iron oxide removal from soils and clays by a dithionite citrate system buffered  
529 with sodium bicarbonate. *Clays clay mineralogy* 7: 317-327

530 OECD Guideline 106 (2000) Adsorption desorption using a batch equilibrium method

531 Papiernik SK, Koskinen WC, Cox L, Rice PJ, Clay SA, Werdin-Pfisterer NR, Norberg KA (2006) Sorption-  
532 desorption of imidacloprid and its metabolites in soil and vadose zone materials. *Journal of agricultural and food*  
533 *chemistry* 54: 8163-8170

534 Patakioutas G, Albanis TA (2002) Adsorption-desorption studies of alachlor, metolachlor, EPTC, chlorothalonil  
535 and pirimiphos-methyl in contrasting soils. *Pest management science* 58: 352-362

536 Postigo C, Barcelo D (2015) Synthetic organic compounds and their transformation products in groundwater:  
537 occurrence, fate and mitigation. *Science of the total environment* 503: 32-47

538 Postle JK, Rheineck BD, Allen PE, Baldock JO, Cook CJ, Zogbaum R, Vandenbrook JP (2004)  
539 Chloroacetanilide herbicide metabolites in Wisconsin groundwater: 2001 survey results. *Environmental science*  
540 *and technology* 38: 5339-5343

541 Pusino A, Liu WP, Gessa C (1992) Influence of organic-matter and its clay complexes on metolachlor  
542 adsorption on soil. *Pesticide Science* 36: 283-286

543 Sanchezcamazano M, Arienzo M, Sanchezmartin MJ, Crisanto T (1995) Effect of different surfactants on the  
544 mobility of selected nonionic pesticides in soil. *Chemosphere* 31: 3793-3801

545 Seybold CA, Mersie W (1996) Adsorption and desorption of atrazine, deethylatrazine, deisopropylatrazine,  
546 hydroxyatrazine, and metolachlor in two soils from Virginia. *Journal of environmental quality* 25: 1179-1185

547 Shaner DL, Brunk G, Belles D, Westra P, Nissen S (2006) Soil dissipation and biological activity of metolachlor  
548 and S-metolachlor in five soils. *Pest Management Science* 62: 617-623

549 Si Y, Takagi K, Iwasaki A, Zhou D (2009) Adsorption, desorption and dissipation of metolachlor in surface and  
550 subsurface soils. *Pest management science* 65: 956-962

551 Sidoli P, Lassabatere L, Angulo-Jaramillo R, Baran N (2016a) Experimental and modeling of the unsaturated  
552 transports of S-metolachlor and its metabolites in glaciofluvial vadose zone solids. *Journal of contaminant*  
553 *hydrology* 190: 1-14

554 Sidoli P, Baran N, Angulo-Jaramillo R (2016b) Glyphosate and AMPA adsorption in soils: laboratory  
555 experiments and pedotransfer rules. *Environmental science and pollution research* 23: 5733-5742

556 Steele GV, Johnson HM, Sandstrom MW, Capel PD, Barbash JE (2008) Occurrence and fate of pesticides in  
557 four contrasting agricultural settings in the United States. *Journal of environmental quality* 37: 1116-1132

558 Tamm O (1922) Eine Methode zur bestimmung der anorganischen Komponenten des Golkomplex in Boden.  
559 *Medd. Statens skogforsoksanst* 19: 385-404.

560 Toccalino PL, Gilliom RJ, Lindsey BD, Rupert MG (2014) Pesticides in groundwater of the United States:  
561 decadal-scale changes, 1993-2011. *Ground water* 52: 112-125,

562 Vryzas Z, Papadopoulou-Mourkidou E, Soulios G, Prodromou K (2007) Kinetics and adsorption of metolachlor  
563 and atrazine and the conversion products (deethylatrazine, deisopropylatrazine, hydroxyatrazine) in the soil  
564 profile of a river basin. *European journal of soil science* 58: 1186-1199

565 Wauchope RD, Yeh S, Linders J, Kloskowski R, Tanaka K, Rubin B, Katayama A, Kordel W, Gerstl Z, Lane M,  
566 Unsworth JB (2002) Pesticide soil sorption parameters: theory, measurement, uses, limitations and reliability.  
567 *Pest management science* 58: 419-445

568 Weber JB, McKinnon EJ, Swain LR (2003) Sorption and mobility of C-14-labeled imazaquin and metolachlor in  
569 four soils as influenced by soil properties. *Journal of agricultural and food chemistry* 51

570 Weber JB, Wilkerson GG, Reinhardt CF (2004) Calculating pesticide sorption coefficients (K<sub>d</sub>) using selected  
571 soil properties. *Chemosphere* 55: 157-166

572 Wood LS, Scott HD, Marx DB, Lavy TL (1987) Variability in sorption coefficients of metolachlor on a captina  
573 silt loam. *Journal of environmental quality* 16: 251-256

574 WRB (2006) World reference base for soil resources 2006. *World Soil*

**Figure 1: Principal component analysis performed on physical and chemical properties measured for soils (samples 1 to 17) and glaciofluvial solids (S-x, Gcm,b[0,2] and Gcm,b]2,10])**

**Figure 2: Partial Least Square-Discriminant analysis of physical and chemical properties for the  $K_d_1$  group,  $K_d_2$  group,  $K_d_3$  group and  $K_d_4$  group defined according to the sorption capacity of soils (samples 1 to 17), and for glaciofluvial solids (S-x, Gcm,b[0,2] and Gcm,b]2,10]) towards metolachlor.**

**Figure 3: Partial Least Square-Discriminant analysis of physical and chemical properties for the  $K_d_1$  group,  $K_d_2$  group,  $K_d_3$  group and  $K_d_4$  group defined according to the sorption capacity of soils (samples 1 to 17), and for glaciofluvial solids (S-x, Gcm,b[0,2] and Gcm,b]2,10]) towards MESA.**

**Figure 4 : Scanning electron microscope (SEM) observations of iron oxides and/or hydroxides (white) on grain surfaces: a) in S-x, b) in Gcm,b[0,2]mm, and c) in Gcm,b ]2,10]mm, as well as d) of clay leaflets on grain surfaces in Gcm,b ]2,10]mm.**

Figure 1

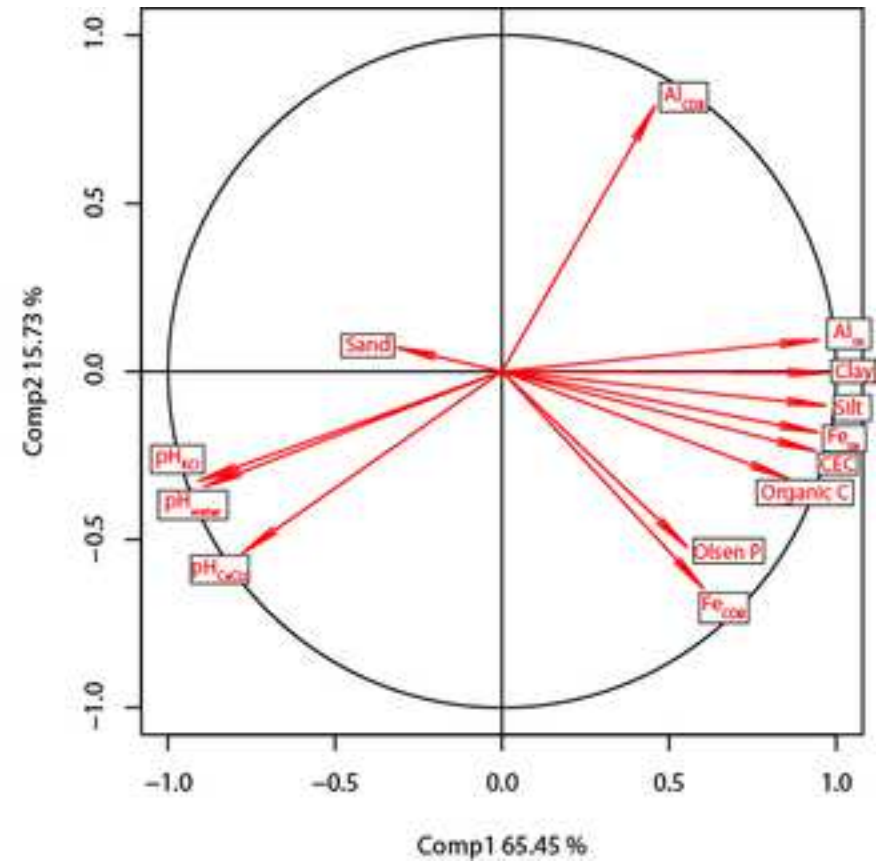
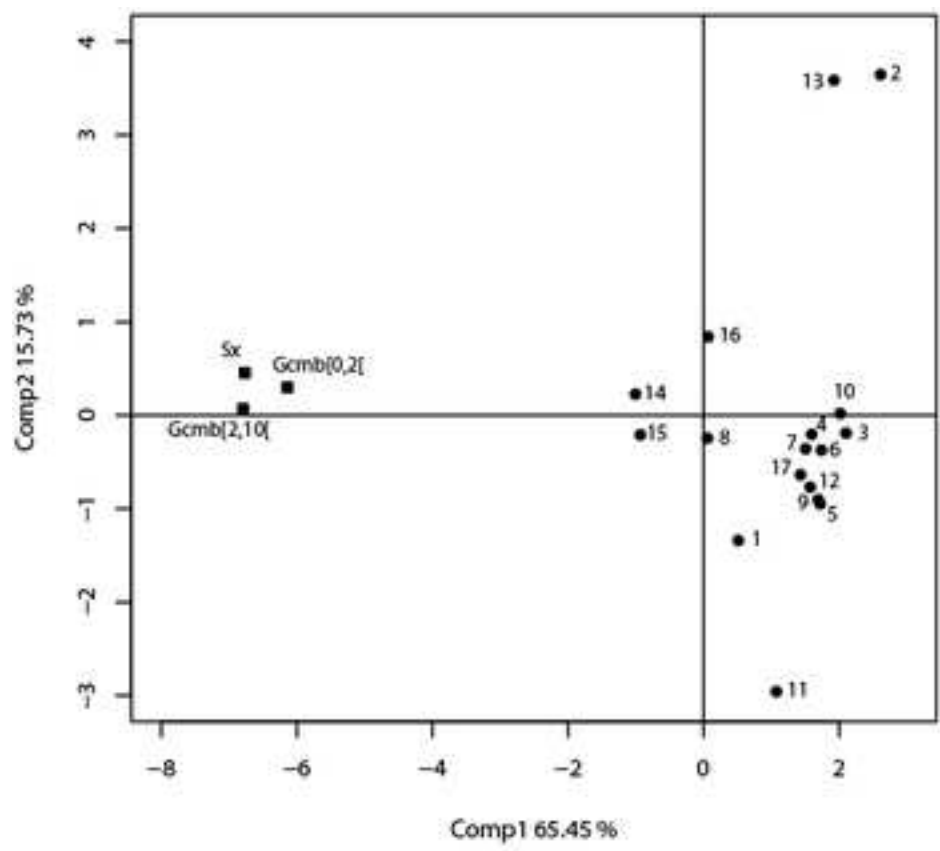


Figure 2

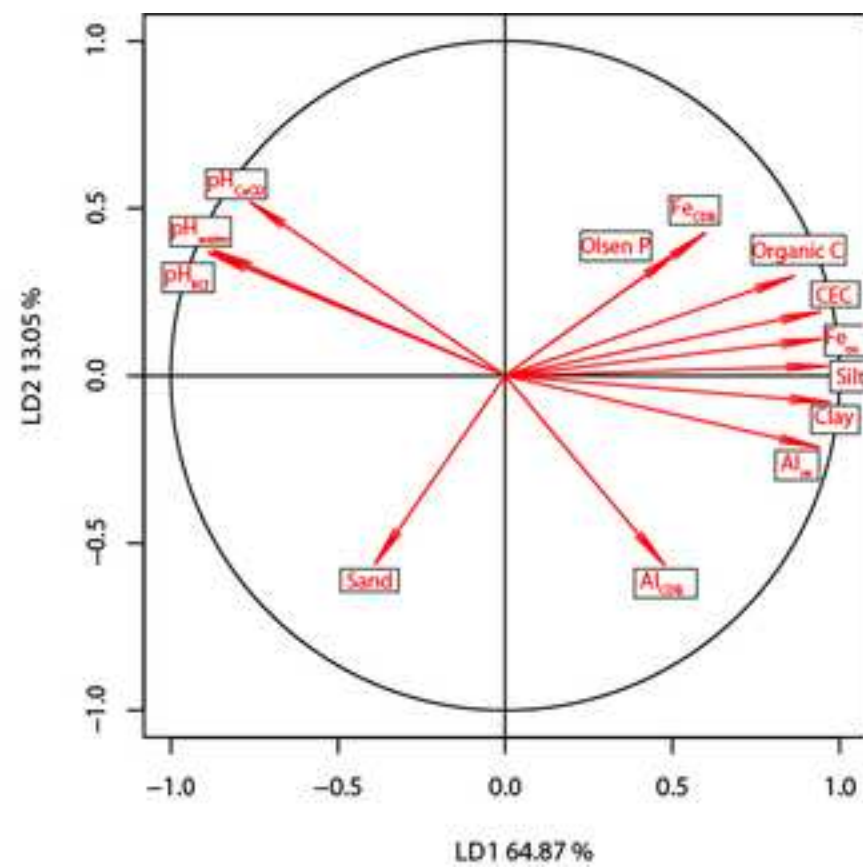
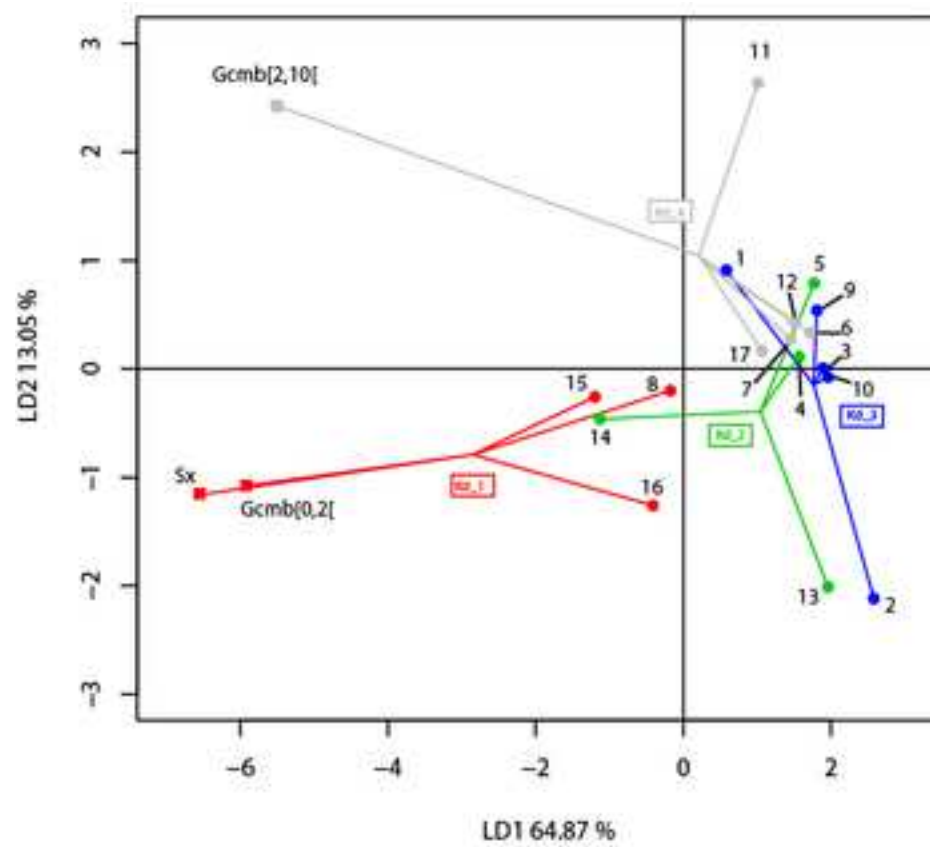
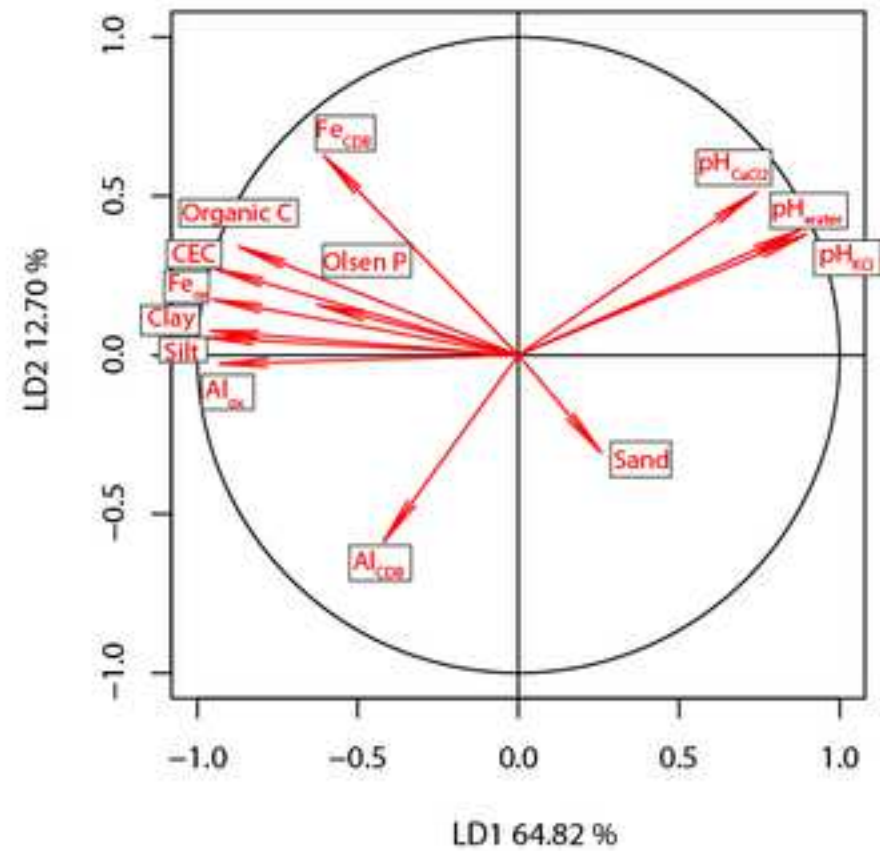
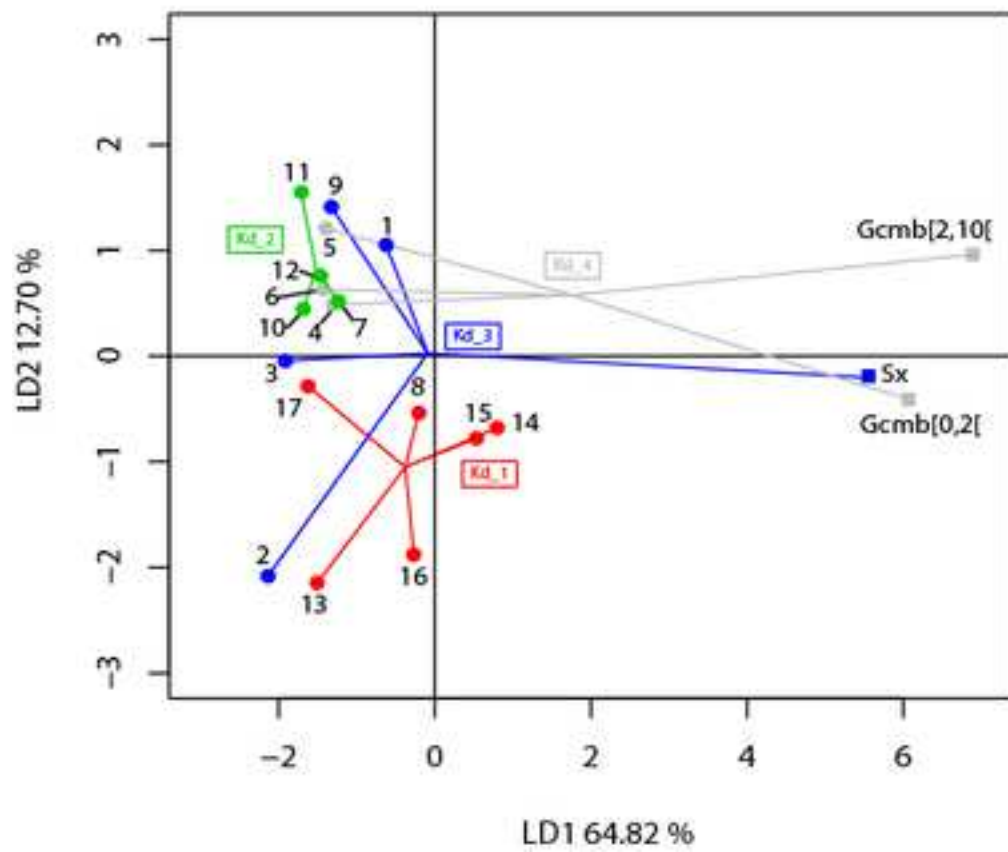
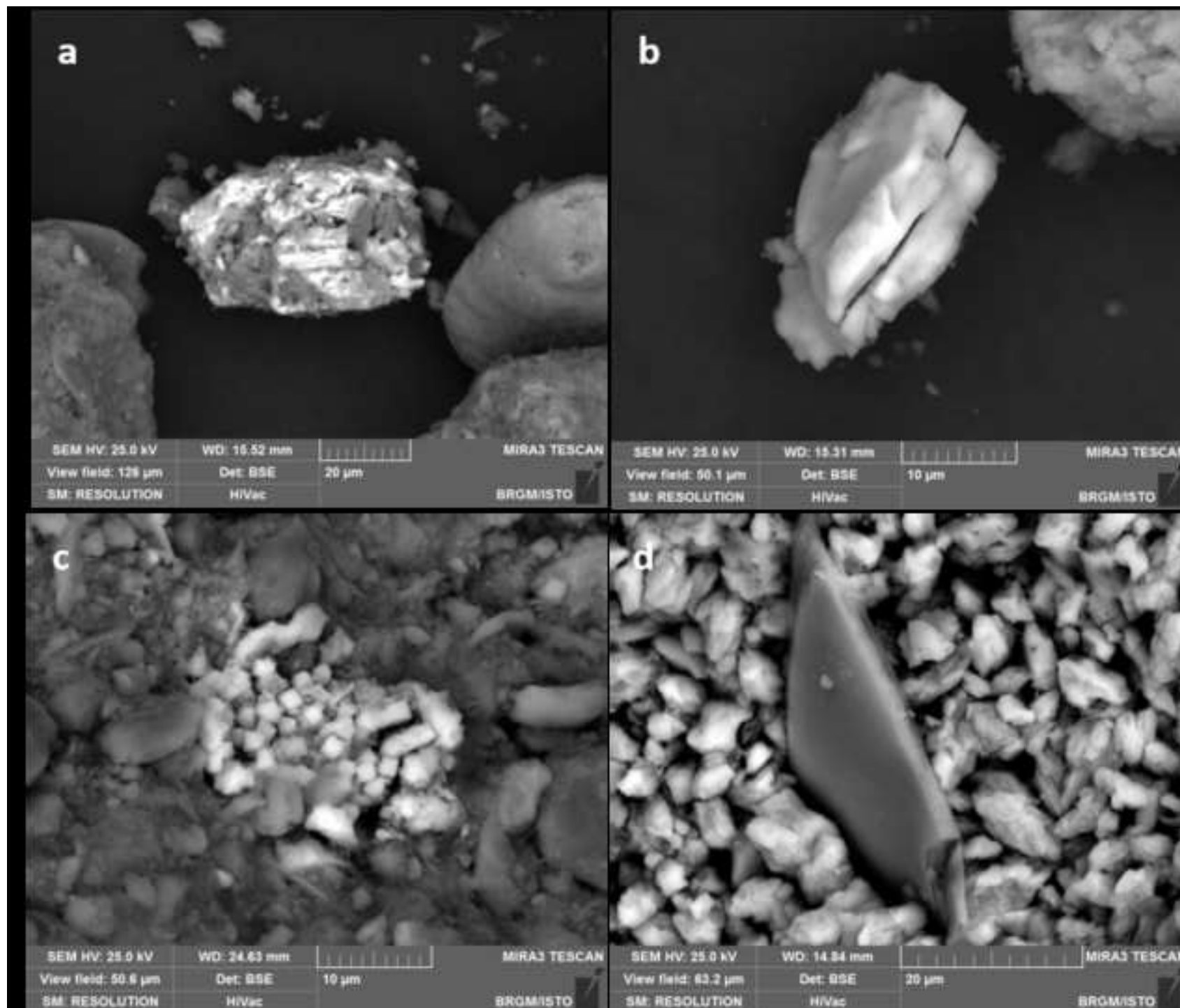


Figure 3





**Table 1: Chemical structures of herbicide S-metolachlor (SMOC) and its anionic metabolites ESA-metolachlor (MESA) and OXA-metolachlor (MOXA)**

Name	S-metolachlor	Metolachlor ESA	Metolachlor OXA
Water solubility (mg/L)	430	212	238
pKa	-	1.8	4.8

**Table 2: Main physical and chemical properties of vadose zone solids**

	pH CaCl <sub>2</sub> a	pH water b	pH KCl c	CEC <sup>d</sup> (meq 100 g <sup>-1</sup> )	%			g kg <sup>-1</sup>						
					Clay	Silt	Sand	Organic C	Olsen P	Al <sub>CDB</sub>	Fe <sub>CDB</sub>	Al <sub>ox</sub>	Fe <sub>ox</sub>	CaCO <sub>3</sub>
<b>Surface soils n=17</b>														
<b>Min</b>	5.1	6.1	4.9	4.4	8.9	29.5	40.8	7.2	0.04	1.5	2.1	1.2	2.1	<1
<b>Max</b>	7.0	8.0	7.2	9.6	15.4	42.3	60.4	23.1	0.20	11.1	13.5	2.2	3.2	<1
<b>Mean</b>	5.9	7.0	6.1	7.4	13.2	36.4	48.4	13.6	0.09	3.1	9.3	1.8	2.7	<1
<b>GFS</b>														
<b>S-x</b>	7.2	9.2	8.8	1.2	2.1	2.2	95.7	2.5	<LQ	0.6	3.0	0.5	0.9	178
<b>Gcm,b [0,2]</b>	7.3	9.1	8.6	1.9	4.2	4.3	91.5	1.1	<LQ	0.7	4.0	0.7	1.2	233
<b>Gcm,b [2,10]</b>	7.3	9.2	8.9	1.1	-	-	-	1.2	<LQ	0.4	3.1	0.0	1.0	356

a pH measured in 1:1 soil/0.01 M CaCl<sub>2</sub> solution (w/w) ratio.

b pH measured in 1:2 soil/water (w/w) ratio.

c pH measured in 1:2 soil/0.01 M KCl solution (w/w) ratio

d Cationic exchange capacity.

n.q. not quantifiable

**Table 3: Mineralogical composition (semi-quantitative XRD analysis) expressed as a percentage of the total of sand (S-x) and both [0,2] and [2,10] bimodal gravel fractions and intra-granular porosity (%)**

	Mineralogical XRD composition										Intra-porosity (%)
	Quartz (±3%)	Calcite (±3%)	Albite (±3%)	Microcline (±3%)	Illite /micas (±5%)	Chlorite (±5%)	Smectite (±5%)	Kaolinite (±5%)	Antigorite (±5%)	Halite (±3%)	
<b>S-x</b>	54	18	7	8	5	3	3	2	-	-	n.q.
<b>Gcm,b [0,2]</b>	36	30	5	4	4	1	13	6	tr.	1	1.5 – 1.6**
<b>Gcm,b [2,10]</b>	32	34	4	5	8	2	7	8	tr.	tr.	1.8±0.2***

n.q. not quantifiable

tr. Traces

\*\* duplicate

\*\*\*triplicate

**Table 4: Values of the  $K_d$  ( $L\ kg^{-1}$ ) distribution constants at equilibrium of SMOC, MESA and MOXA measured on the ZNS solids. Average values of the experimental triplicates for an initial doping concentration of 1 mg/L.**

		mean $K_d$ SMOC	mean $K_d$ MESA	mean $K_d$ MOXA
<b><u>Surface soils</u></b>				
	<b>1</b>	4.23	0.23	n.q.
	<b>2</b>	4.01	0.35	n.q.
	<b>3</b>	4.01	0.40	n.q.
	<b>4</b>	3.63	0.52	n.q.
	<b>5</b>	3.90	0.70	n.q.
	<b>6</b>	4.97	0.74	n.q.
	<b>7</b>	4.74	0.17	n.q.
	<b>8</b>	2.34	0.05	n.q.
	<b>9</b>	4.21	0.27	n.q.
	<b>10</b>	4.36	0.15	n.q.
	<b>11</b>	6.32	0.10	n.q.
	<b>12</b>	4.46	0.06	n.q.
	<b>13</b>	3.50	0.03	n.q.
	<b>14</b>	3.30	0.04	n.q.
	<b>15</b>	2.84	n.q.	n.q.
	<b>16</b>	2.90	0.04	n.q.
	<b>17</b>	5.60	0.05	n.q.
<b><u>GFS</u></b>				
	<b>S-x</b>	0.44	0.73	n.q.
	<b>Gcm,b [0-2] mm</b>	0.57	0.46	n.q.
	<b>Gcm,b ]2-10] mm</b>	28.8	2.08	0,74

n.q. not quantifiable